Supporting information

Low-loss Optical Waveguide from 1D Europium Nanocluster

Jingjing Xia,[a,‡] Weinan Dong,[a‡] Shengrong He,[a] Feng Jiang,[a,*] Wenming Tian,[b,*] Qi Sun,[b] Meixin Hong,[a] Lingchen Meng,[a] Yu Zhang,[a] Zhennan Wu,[a,*] Tingting Li,[c,*] Xue Bai,[a,*]

[a]State Key Laboratory of Integrated Optoelectronics, JLU Region, College of Electronic Science and Engineering, Jilin University, 2699 Qianjin Street, Changchun, 130012, P. R. China.
[b]State Key Laboratory of Molecular Reaction Dynamics, Dalian Institute of Chemical Physics, Chinese Academy of Sciences, 457 Zhong Shan Road, Dalian 116023, P. R. China.
[c]College of Materials Science and Engineering, Jilin Jianzhu University, Changchun 130012, P. R. China

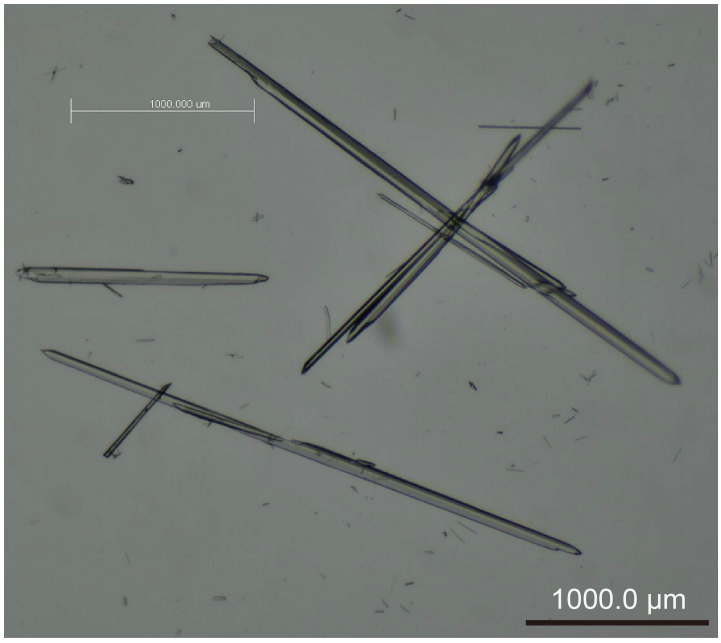

Figure S1. Crystal morphology: Needle-rod-like macroscopic morphology of Eu-NC under optical microscope.

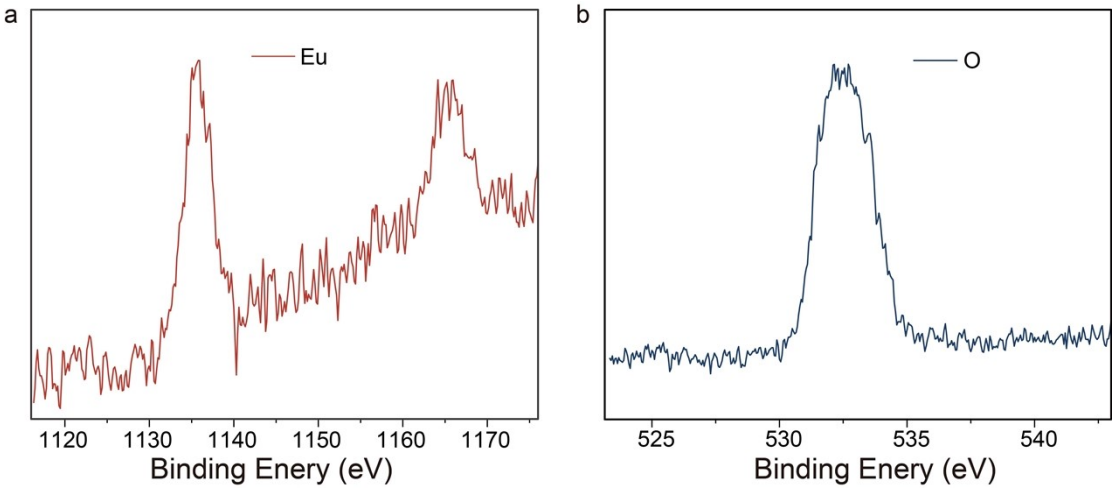

Figure S2. The X-ray photoelectron spectroscopy of Eu-NC. The binding energy peaks at 1130-1170 eV corresponding to Eu^{3+} (a) and 529-535 eV corresponding to O^{2-} (b) respectively.

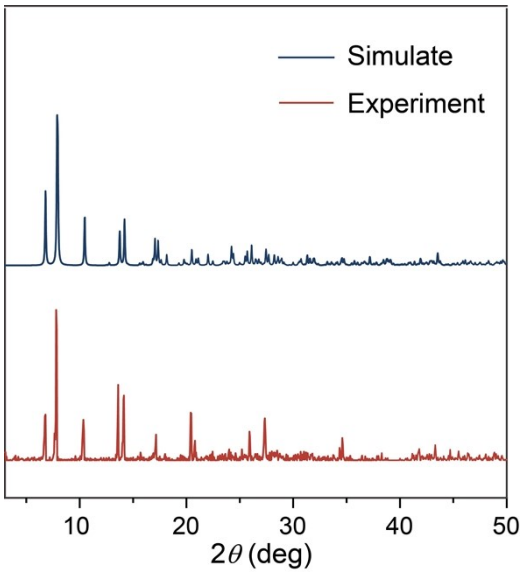

Figure S3. Powder X-ray diffraction pattern (PXRD) for Eu-NC. The PXRD of the crystal is well indexed to the standard card of Eu-NC, indicating the formation of high-purity solid without any impurity phases.

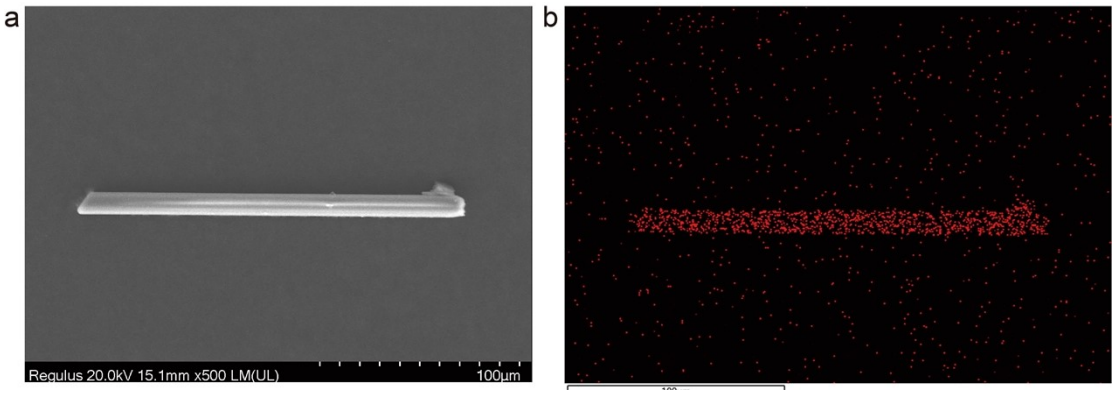

Figure S4. Scanning Electron Microscope Testing: (a) SEM image of the as-prepared Eu-NC. (b) EDX mapping of Eu-NC.

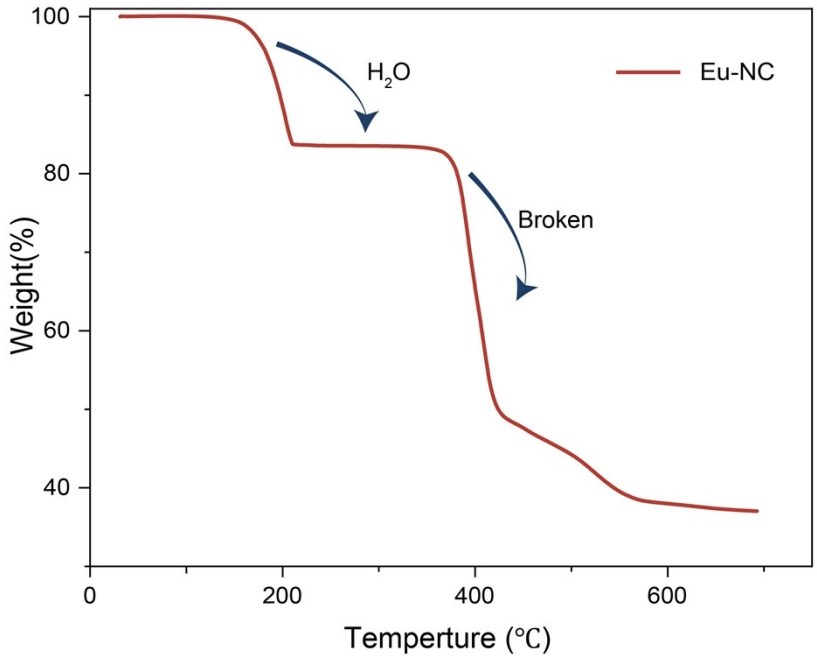

Figure S5. The TGA curves of Eu-NC under nitrogen-containing conditions.

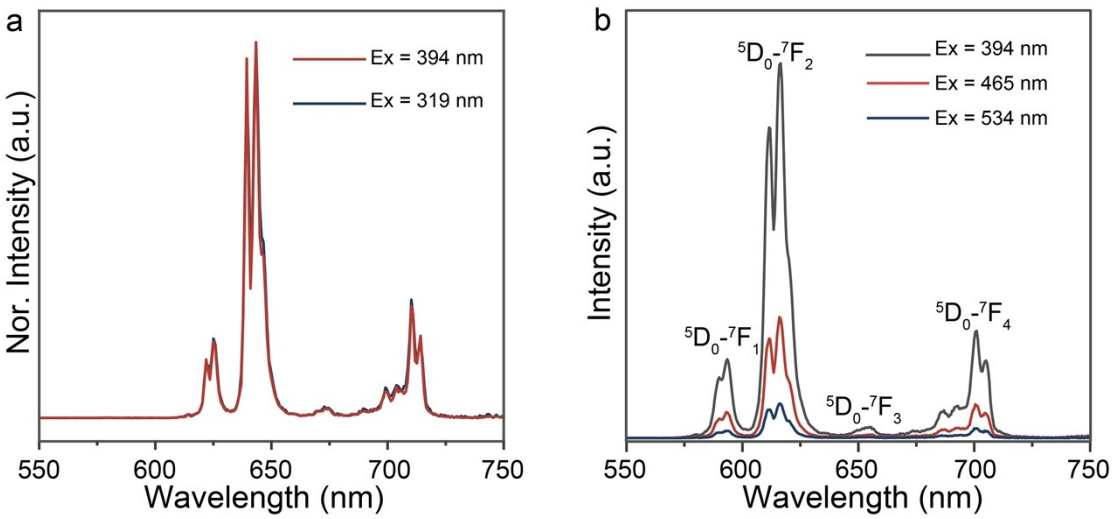

Figure S6. Variable-excitation emission spectrum. (a) Normalized emission spectra of Eu-NC upon ligand-directed excitation (319 nm) and Eu^{3+} intrinsic excitation (394 nm) under ambient conditions. (b) Emission spectra of Eu-NC under different intrinsic excitations.

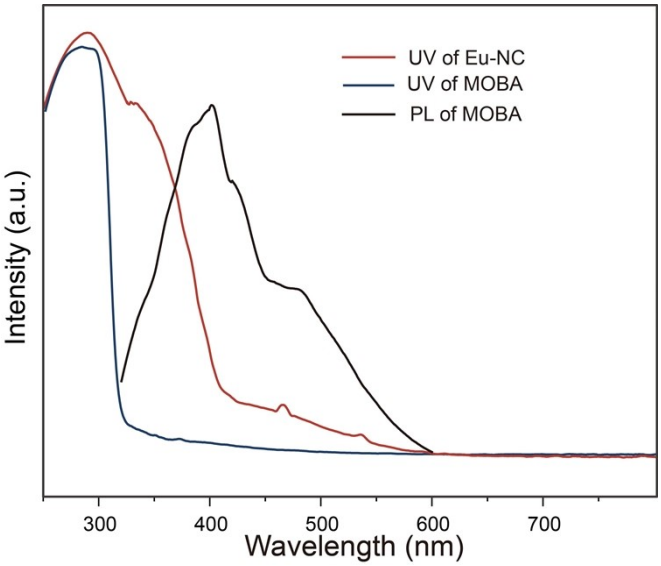

Figure S7. Solid-state UV-VIS spectra of Eu-NC (red line) and MOBA (blue line) at room temperature; emission spectra of MOBA (black line) at room temperature. The absorption peak of Eu-NC completely overlaps with that of MOBA and exhibits the characteristic absorption peak of Eu^{3+}; the emission peak of MOBA is around 412 nm.

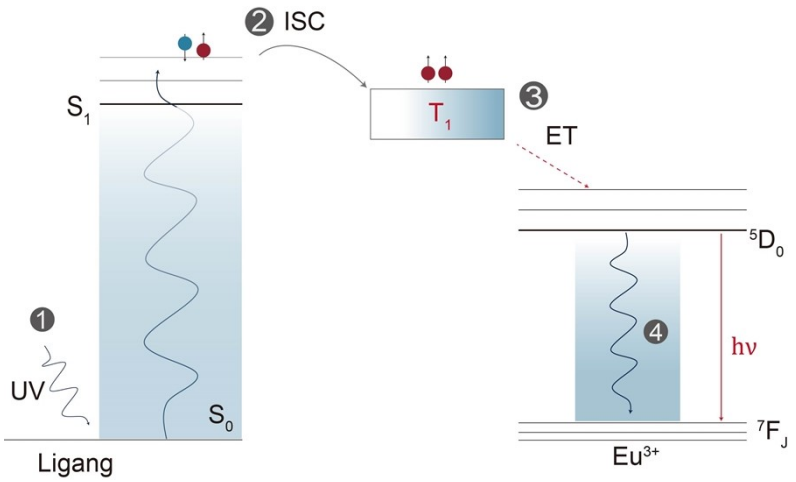

Figure S8. The process of intramolecular energy transfer from the ligands to Eu^{3+} centers. ***1.*** represents the process of ultraviolet light excitation of ligands, the electron transitions from the ground state S_0 of the ligand to the first excited singlet state S_1, ***2.*** indicates the transfer of electrons to the triplet state via intersystem crossing (ISC), ***3.*** represents the transfer of energy to rare-earth ions via non-radiative energy transfer (ET), placing them in an excited state, ***4.*** indicates that rare-earth ions emit light through radiative transitions.

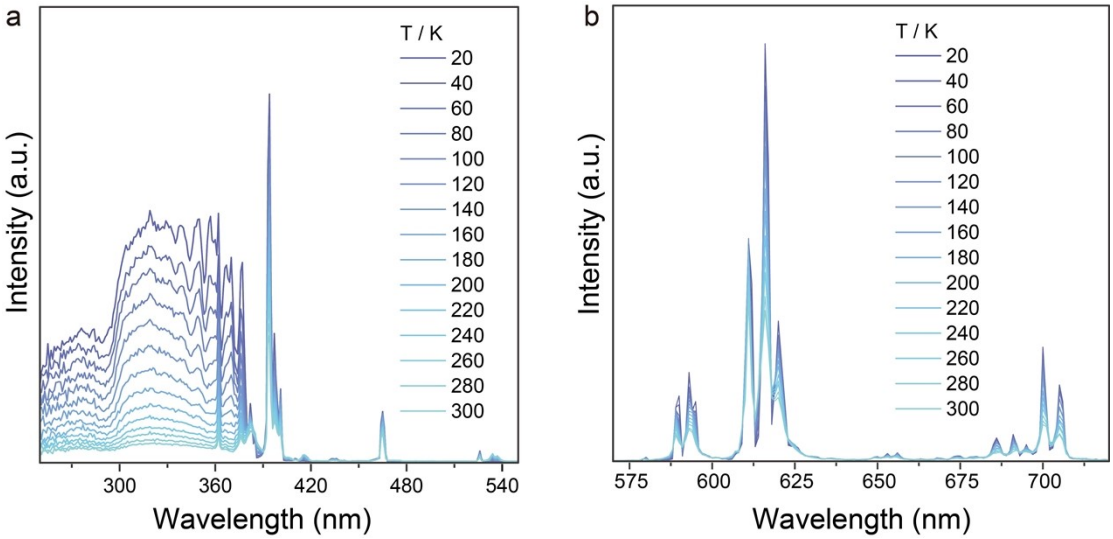

Figure S9. Variable-temperature spectroscopy testing from 20K to 300K. (a) Excitation spectrum of Eu-NC under emission at 616 nm. (b) Emission spectrum of Eu-NC under excitation at 319 nm.

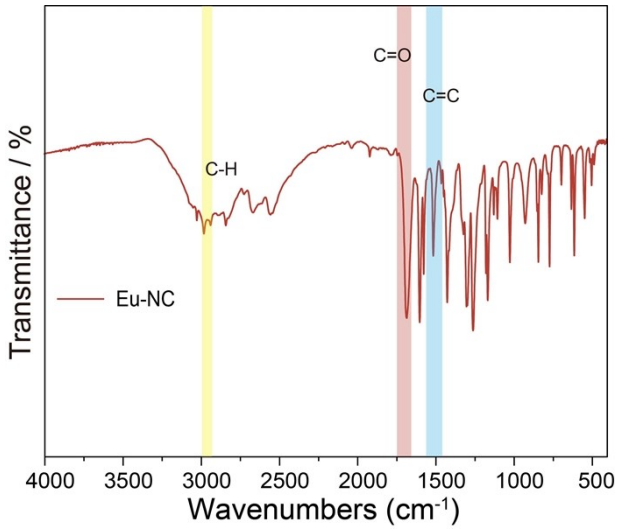

Figure S10. Infrared Spectra of Eu-NC among 500-4000 cm^{-1}. The strong absorption bands from 1750 cm^{-1} and 1620 cm^{-1} were caused by the C=O, C=C vibration of MOBA. The absorption band at 2900 cm^{-1} is caused by C-H vibrations.

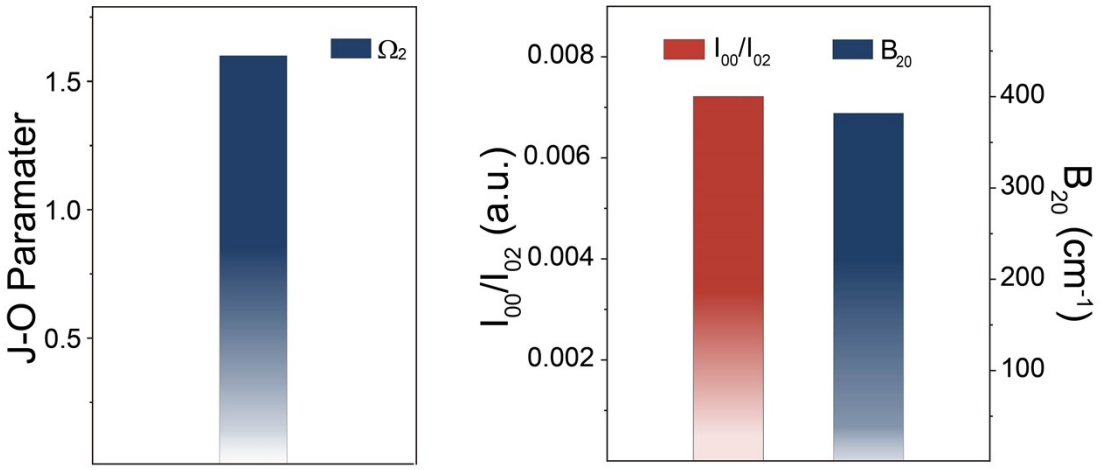

Figure S11. Judd-Ofelt intensity parameters Ω_2 of Eu-NC and the second-order crystal field parameter analysis for Eu-NC.

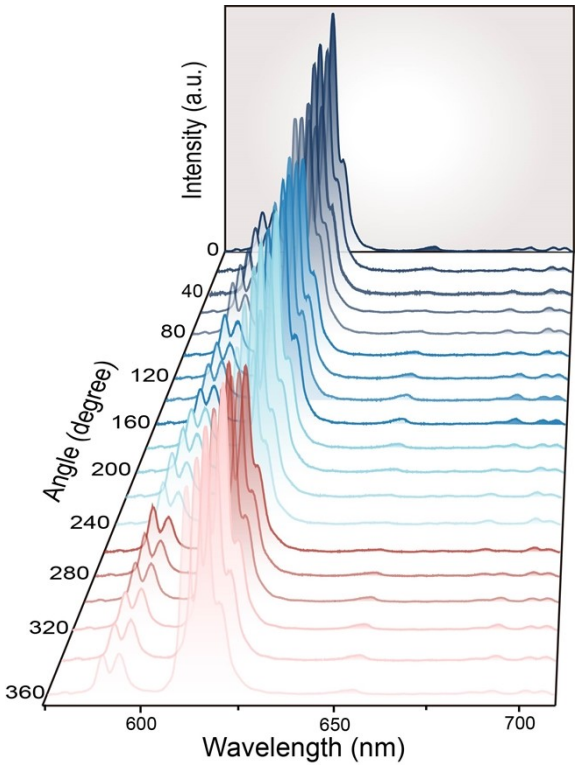

Figure S12. Polarized PL spectrum of Eu-NC microrod at variable angles (0~360°).

Table S1. Crystallographic data for compounds Eu-NC.

Compound	Eu-NC
Formula	C24H21EuO9
FW	605.37
T/K	100
Cry. system	monoclinic
Space group	P21/c
a /Å	13.40601(4)
b /Å	22.2215(4)
c /Å	7.6893(5)
α /o	90(2)
β /o	104.4150(2)
γ /o	90(3)
V/Å3	2218.54(17)
Z	4
Dc/g cm–3	1.812
μ/ mm–1	2.881
Data/parameters	5085/310
2θ/o	5.77-55.02
F(000)	1200.0
GOF	1.127
R1[I> 2σ(I)]a	0.0159
wR2(All data)b	0.0373